

## Review Article

# Contemporary Physical Methods in Studies of Lipid Phase Polymorphism

Meiyi Li<sup>1</sup>, Edward S. Gasanoff<sup>1</sup>

1. STEM Research Center, Chaoyang KaiWen Academy, China, Beijing

Lipid polymorphism is a well-documented phenomenon reported both in model lipid membranes and biological membranes. Elucidation of the role of lipid polymorphism and the role of non-bilayer lipid structures is a rapidly developing field of research studies focused on structure and function relationships in membranes of cells and intracellular organelles. The development of this area of research largely depends on application of powerful physical methods which allow one to ‘see’ dynamic transitions in structure of lipid phase at various time scales. In this review we describe the application of nuclear magnetic resonance (NMR), electron paramagnetic resonance (EPR), and luminescence spectroscopy, and differential scanning microcalorimetry in analysis of polymorphic transitions in lipid phase of model and biological membranes.

## Introduction

In this work we outline the advantages of powerful contemporary physical methods employed in studies of dynamic structure of non-bilayer lipid phases in model and biological membranes. We also critically review the important experimental and theoretical research data which became available over the past sixty years on dynamics and structure of non-bilayer lipid phases in model membranes and the effects of non-bilayer phases on functional activities of biological in order to propose the structural and functional roles which non-bilayer lipid phases play in physiological activities of biological membranes.

Although the methods of X-ray diffraction microscopy such as small-angle X-ray diffraction and freeze-fracture electron microscopy were one of the first methods which reported existence of non-bilayer lipid phases [\[1\]\[2\]\[3\]\[4\]\[5\]\[6\]\[7\]](#), we will not review these methods in this chapter as these methods do not reflect dynamic processes as they offer a ‘static picture’ of structural features of

membranes treated at temperatures greatly lower than physiological temperatures. In this chapter we briefly describe the principles of methods which provide key information on dynamic changes in membrane polymorphism, intermembrane lipid exchange and membrane fusion that should help readers better understand the proposed mechanisms on how non-bilayer phases regulate bioenergetics of thylakoid and mitochondrial membranes.

## **<sup>31</sup>P-NMR spectroscopy**

<sup>31</sup>P-nuclear magnetic resonance (<sup>31</sup>P-NMR) spectroscopy is a powerful and non-invasive method to investigate dynamics and morphological organization of bulk phospholipids in model and biological membranes in the time scale of  $10^{-2}$ – $10^{-4}$  s [8]. Phospholipids with restricted mobility caused by direct binding of phospholipids to the surface of intrinsic membrane proteins (annular phospholipids) or to the proteins' hydrophobic grooves and cavities are 'invisible' to <sup>31</sup>P-NMR as the molecular mobility of these phospholipids is slower than the  $10^{-2}$ – $10^{-4}$  s time range [9]. Thus, <sup>31</sup>P-NMR spectroscopy allows to study bilayer to non-bilayer lipid phase polymorphic transitions of bulk phospholipids which could be then related to functional activities of biological membranes.

<sup>31</sup>P-NMR spectrum line shape depends on orientation of phosphodiester bonds of phospholipids in the applied magnetic field [10]. In a lamellar phase, in which phospholipids are arranged in a bilayer packing, orientation of phosphodiester bonds in applied magnetic field is anisotropic which results in <sup>31</sup>P-NMR spectrum with a characteristic 'bilayer' line shape (Figure 1).

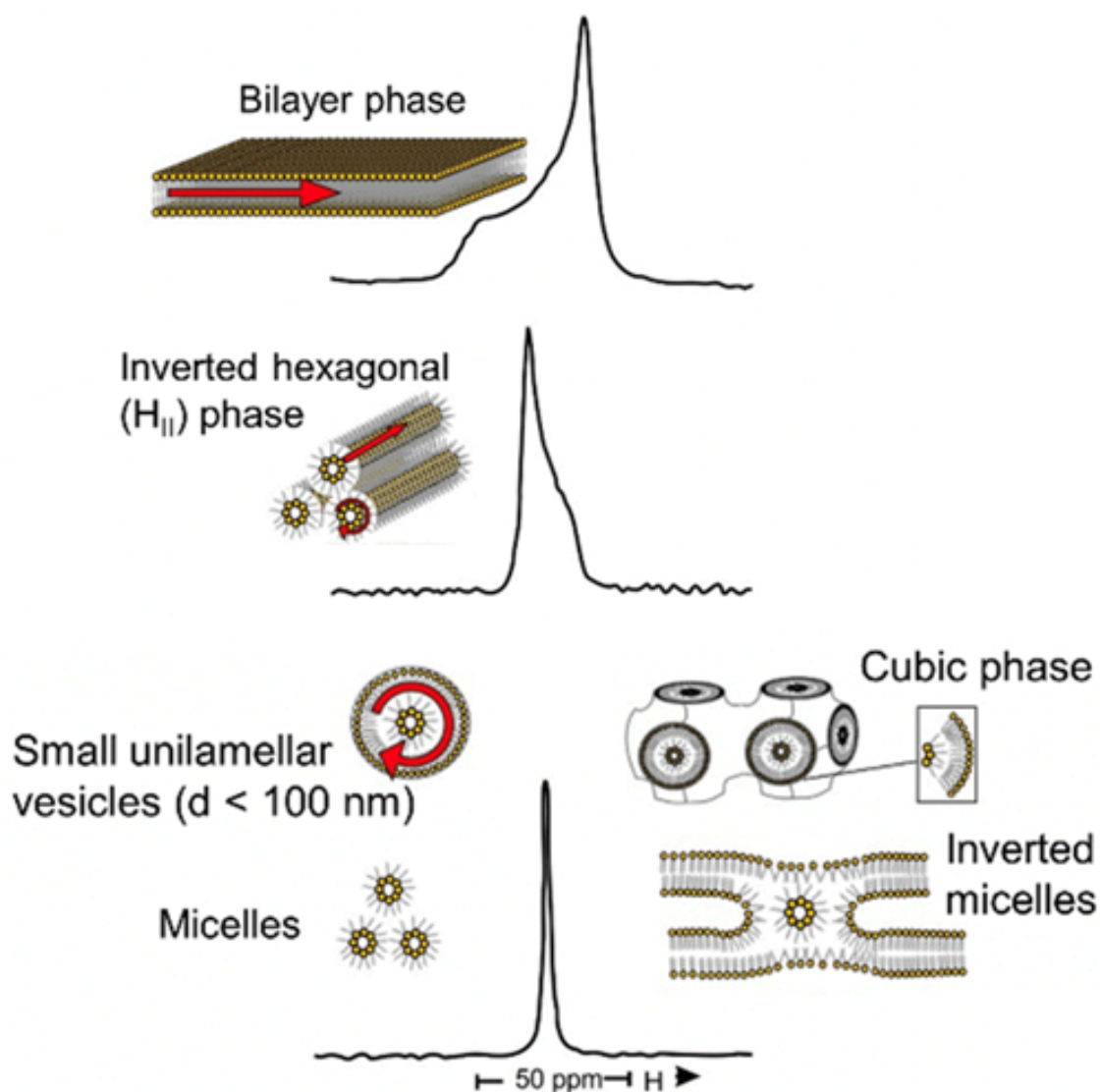


**Figure 1.**  $^{31}\text{P}$ -NMR spectrum line shape signatures according to [10]. This figure is modified from [7]. In the hexagonal  $H_{II}$  phase, phospholipids are arranged in one of the non-bilayer forms and packed in a system of tubular inverted micelles in which anisotropic orientation of phosphodiester bonds in applied magnetic field lays along the long axes of inverted micellular tubes resulting in a characteristic  $^{31}\text{P}$ -NMR line shape of the hexagonal  $H_{II}$  phase (Figure 1). In the other forms of non-bilayer lipid phases shown in Figure 1, orientation of phosphodiester bonds in applied magnetic field is isotropic which generates very narrow 'isotropic'  $^{31}\text{P}$ -NMR line shape.

## **$^1\text{H}$ -NMR spectroscopy**

$^1\text{H}$ -NMR spectroscopy has been used extensively in studies of membrane permeability of unilamellar phosphatidylcholine liposomes in aqueous solutions of ferricyanide ions  $[\text{Fe}(\text{CN})_6]^{3-}$  [11][12][13][14]. Membranes of intact unilamellar liposomes are not permeable to the paramagnetic ions  $[\text{Fe}(\text{CN})_6]^{3-}$  [11][12]. When ferricyanide ions interact with the choline group  $\text{N}^+(\text{CH}_3)_3$  of phosphatidylcholine (PC), the  $^1\text{H}$ -NMR signal of choline group of PC on the outer monolayer of liposomal membrane shifts towards a stronger magnetic field, but the  $^1\text{H}$ -NMR signal of choline group of PC on the inner monolayer of liposome does not shift to a stronger field as  $[\text{Fe}(\text{CN})_6]^{3-}$  ions cannot reach into the inner volume of liposomes as long as liposome membranes remain impermeable to  $[\text{Fe}(\text{CN})_6]^{3-}$  ions. This causes the split the  $^1\text{H}$ -NMR signals of choline groups from outer and inner monolayer with intensity of signal from outer monolayer being bigger than that of inner monolayer (Figure 2 – bottom spectra).

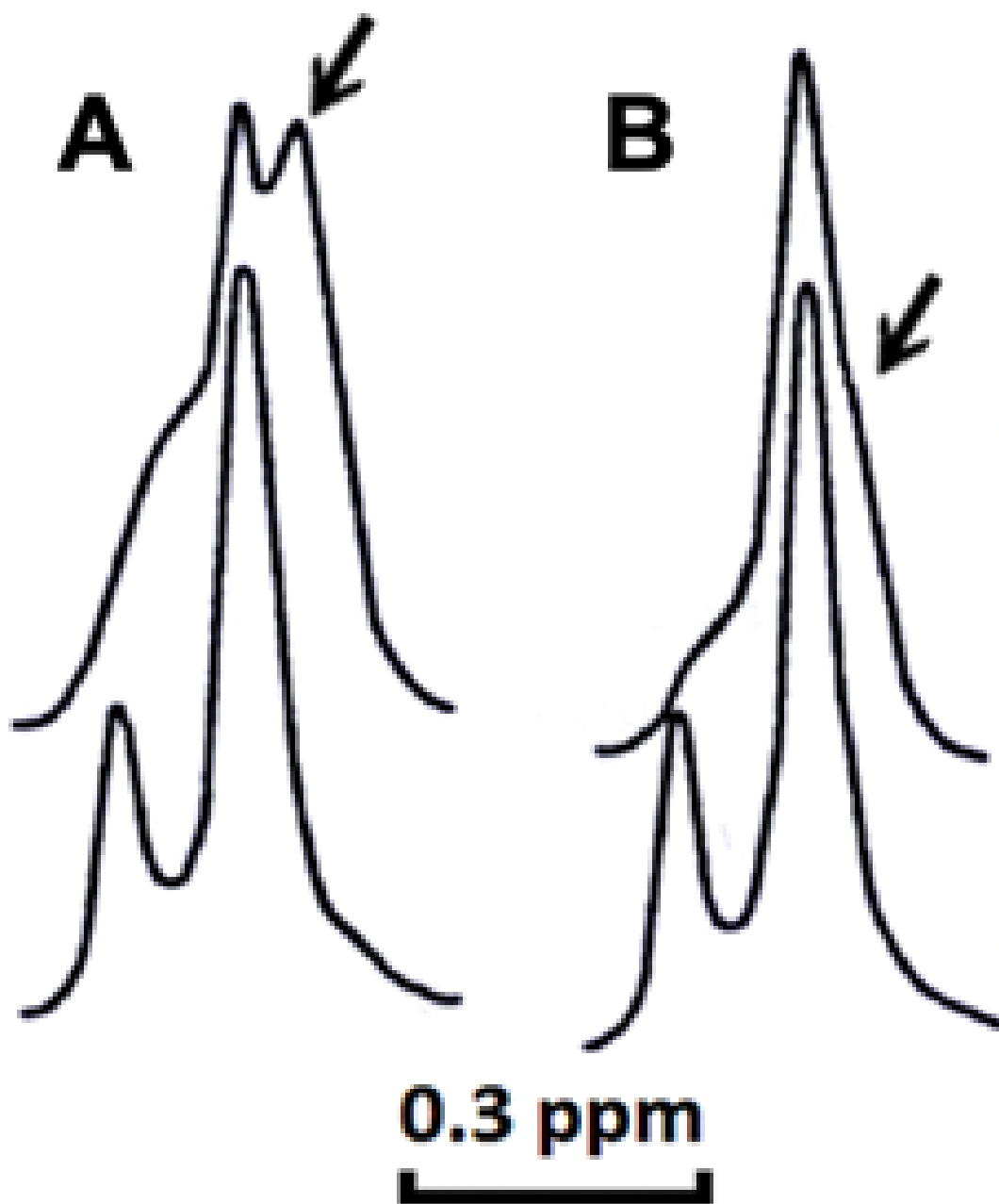


**Figure 2.** <sup>1</sup>H-NMR spectra of the N<sup>+</sup>(CH<sub>3</sub>)<sub>3</sub> groups of PC in unilamellar liposomes composed of PC+ 10 mol% cardiolipin (A) and PC+ 10 mol% phosphatidylserine (B) in the presence of K<sub>3</sub>[Fe (CN)<sub>6</sub>]<sub>3</sub> in samples of untreated liposomes (bottom spectra) and liposomes treated with cobra venom cytotoxin which phenocopies C8 subunit of the F<sub>0</sub> sector in bovine ATP synthase at a cytotoxin: lipid molar ratio of 0.02 (top spectra). The arrows point at the signals from non-bilayer phase. This figure is modified from <sup>[13]</sup>.

Treatment of PC liposomes containing 10 mol% of phosphatidylserine (PS) with cobra venom cytotoxin, a protein which phenocopies some biophysical and biochemical properties of C8 subunit of the  $F_0$  sector in bovine ATP synthase [15], results in disappearance of  $^1\text{H}$ -NMR signal from inner monolayer (Figure 2B top spectrum). This happens because cytotoxin disturbs structural integrity of liposomal membrane made of PC + PS making it permeable to  $[\text{Fe}(\text{CN})_6]^{3-}$  ions which can now reach into the inner volume and react with  $\text{N}^+(\text{CH}_3)_3$  groups of PC on the inner monolayer shifting the  $^1\text{H}$ -NMR signal to the stronger field. Thus,  $\text{N}^+(\text{CH}_3)_3$  groups from outer and inner monolayers resonate now at the same frequency. Treatment with cytotoxin of PC liposomes containing 10 mol% of cardiolipin (CL) generates a new signal on a high field side from a signal of choline groups on outer monolayer (Figure 2A top spectrum – see arrow). This new high field signal comes from the non-bilayer lipid phase in which choline groups of PC react at a closer distance with  $[\text{Fe}(\text{CN})_6]^{3-}$  ions. The shoulder like line on a low field side from a signal of choline groups from outer monolayer is an extension of signal from non-bilayer lipid phase (Figure 2A top spectrum). Thus the  $^1\text{H}$ -NMR spectrum line from the cytotoxin-treated PC+CL liposomes is the superposition of signals from bilayer and non-bilayer lipid phases (Figure 2A top spectrum). A small amount of non-bilayer lipid phase could be also detected in the cytotoxin-treated PC+PS liposomes from the slightly visible hump (see arrow in Figure 2B top spectrum) on a high field side from a signal of choline groups on outer monolayer and a shoulder like line on a low field side.

## **$^2\text{H}$ -NMR spectroscopy**

$^2\text{H}$ -NMR spectroscopy has been used to study the orientation and movement of  $^2\text{H}_2\text{O}$  bound to lipid membrane surface [12][13][16]. Water molecules bound to lipid headgroups via ion-dipole and/or dipole-dipole forces of attraction are restricted to lateral anisotropic movement along the membrane bilayer surface that generates a characteristic quadrupole splitting of a  $^2\text{H}$ -NMR resonance line (Figure 3A). The value of quadrupole splitting of the  $^2\text{H}$ -NMR resonance line is directly proportional to the degree of anisotropic movement [16] which is different for different lipid phases. Polymorphic transition from the bilayer lipid phase to non-bilayer phase is associated with the change from anisotropic movement of the lipid-bound water molecules to isotropic movement of lipid-bound water molecules [12].

The  $^2\text{H}$ -NMR spectrum with an axially symmetrical tensor of the electrical field gradient was yielded from the sample of PC membranes containing 10 mol% cardiolipin and hydrated at the molar ratio  $^2\text{H}_2\text{O}$  to lipid 10: 1 (Figure 3A). The value of quadrupole splitting of this spectrum was 1050 Hz that points to anisotropic movement of water bound to surface of bilayer membrane, however this is significantly smaller of the quadrupole splitting value of water in ice (16500 Hz <sup>[17]</sup>) where molecular movement is limited only to vibration. Treatment of the hydrated membrane made of PC+10 mol% CL with cytotoxin CTI at a molar ratio  $^2\text{H}_2\text{O}$ : CTI: lipid = 100: 1: 10 resulted in the  $^2\text{H}$ -NMR spectral line which is a superposition of duplet and singlet signals (Figure 3B). A singlet signal comes from isotropically oriented water molecules bound to lipids of non-bilayer phase which is triggered by and physically associated with cytotoxin CTI <sup>[12]</sup>. It has been suggested that a singlet signal may also come from water molecules bound to the cytotoxin's molecular surface where water molecules are isotropically oriented <sup>[13]</sup>. This implies that cytotoxin CTI removes water from membrane surface resulting in dehydration of certain areas on membrane surface <sup>[12][13]</sup>. Caused by treatment with cytotoxin CTI, the value of quadrupole splitting of a duplet signal fell down from 1050 Hz to 700 Hz which may reflect on an increase in plasticity of bilayer membrane and facilitated exchange of water molecules between still hydrated and already dehydrated areas on membrane surface <sup>[12]</sup>. Treatment of PC+10 mol% CL membrane with cytotoxin CTII at a molar ratio  $^2\text{H}_2\text{O}$ : CTII: lipid = 100: 1: 10 also generated the  $^2\text{H}$ -NMR spectral line which is a superposition of duplet and singlet signals (Figure 3C). However, with CTII, the decrease in the value of quadrupole splitting of a duplet signal was greater than that with CTI – the decrease with CTII was from 1050 Hz to 540 Hz. This indicates that CTII is more capable than CTI in triggering formation of non-bilayer lipid phase in PC membranes containing CL which agrees well with the plethora of previous experimental research conducted with CTI and CTII <sup>[18][12][13][14][15][19][20][21]</sup>.

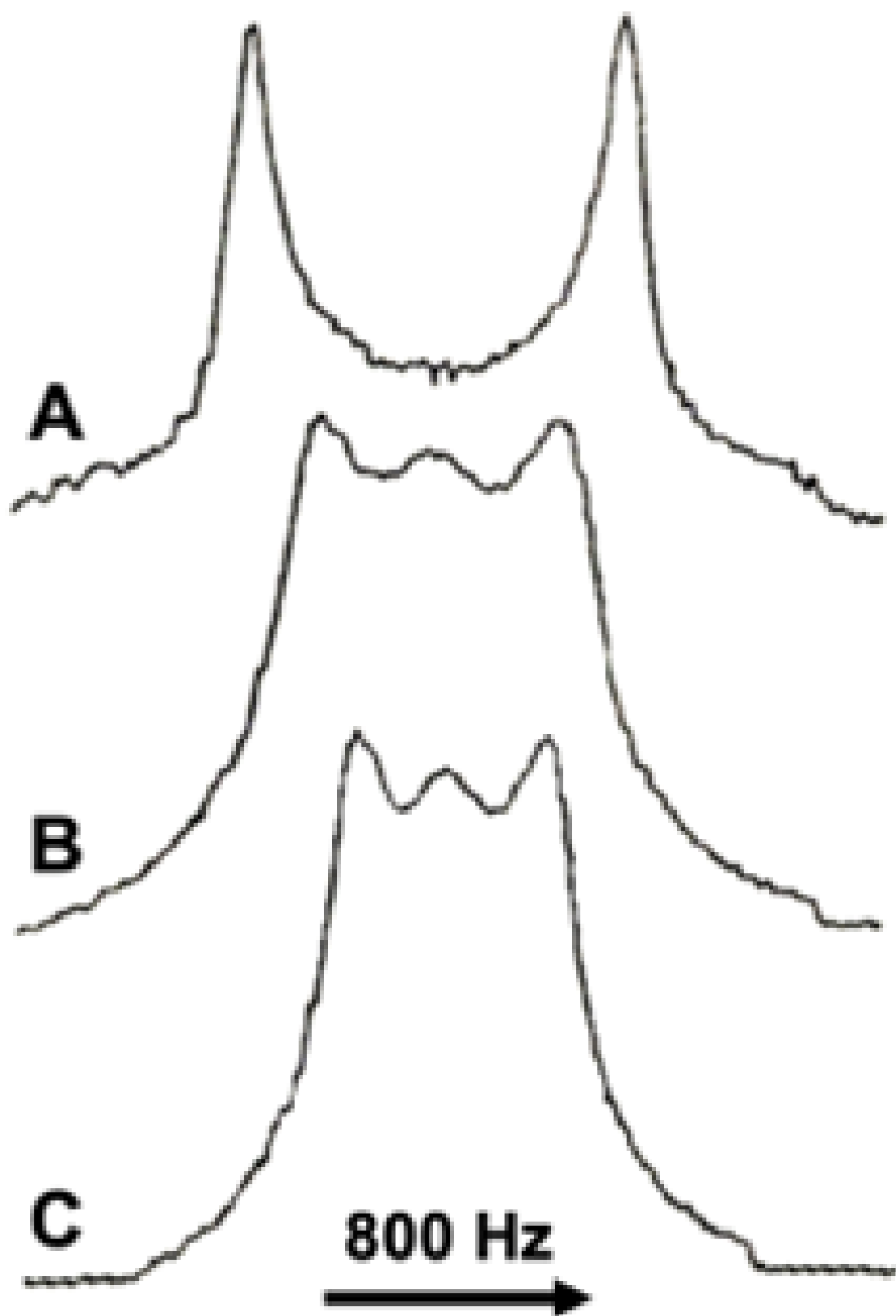


Figure 3.  $^2\text{H}$ -NMR spectra of  $^2\text{H}_2\text{O}$  bound to the surface of untreated unilamellar liposomes composed of PC+10 mol% CL (A), liposomes of same composition treated with cytotoxin CTI (B) and with cytotoxin



## EPR spectroscopy of spin probes in oriented multi-bilayer lipid films

Electron paramagnetic resonance (EPR) spectroscopy of spin labels with a hydrophobic alkyl chain is a biophysical method widely used to study rotational and lateral movement of lipids in model and biological membranes in the  $10^{-6}$ - $10^{-11}$  s time scale [22][23]. The 4,4-dimethyl-3-oxazolinyl (DOXYL) group attached to selected carbon atom along the alkyl chain of stearic acid makes an excellent spin label to study changes in molecular organization and membrane fluidity in hydrophobic area of membrane [23]. In EPR spectroscopy in oriented lipid films, hydrated lipids with doxyl-stearic acid (DSA) are squeezed between the glass plates into the bilayer lipid films at molar ratio lipid: DSA = 100: 1. The long molecular axis of DSA aligns along the normal to the bilayer lipid surface and generates high resolution EPR spectra that demonstrate strong angular anisotropy at different orientations of the lipid film normal in the applied magnetic field. EPR spectrum of 5-DSA (doxyl group attached to the fifth carbon atom of alkyl chain) in lipid film of PC+10 mol% PS in absence of cytotoxin has a narrow EPR spectral line at a perpendicular orientation of the bilayer normal in the magnetic field and a wide spectral line at parallel orientation of the bilayer normal in the magnetic field (Figure 4). This high angular spectral anisotropy represented by non-superimposed EPR spectral lines at different orientations of lipid film in magnetic field points to the highly ordered packing of lipids in the lamellar phase. Angular anisotropy of EPR spectra of lipid film treated with CTII at cytotoxin/lipid molar ratio = 0.02 has decreased as the resonance line at perpendicular orientation of the bilayer normal in magnetic field has broadened and resonance lines at different orientations partially overlapped (Figure 4A). At the CTII/lipid molar ratio 0.04, the EPR spectra of lipid film showed virtually complete angular isotropy as the spectral lines at different orientations of lipid film normal in magnetic field are nearly completely superimposed (Figure 4A). Spectral isotropy of resonance lines at different orientations of the lipid film normal in magnetic field strongly suggests the high degree of disorder in lipid packing – a result of polymorphic transition from lamellar to non-bilayer lipid phase. Treatment of the same lipid film with CTI at a gradually increasing cytotoxin concentrations did disturb spectral anisotropy of EPR spectral lines but did not lead to superimposition of spectral lines derived from different orientations of the lipid film normal with

respect to the direction of magnetic field (Figure 4B). This observation suggests that CTI does disturb parking of lipids in PC+10 mol% PS membrane but does not cause polymorphic transition from bilayer to non-bilayer lipid phase.

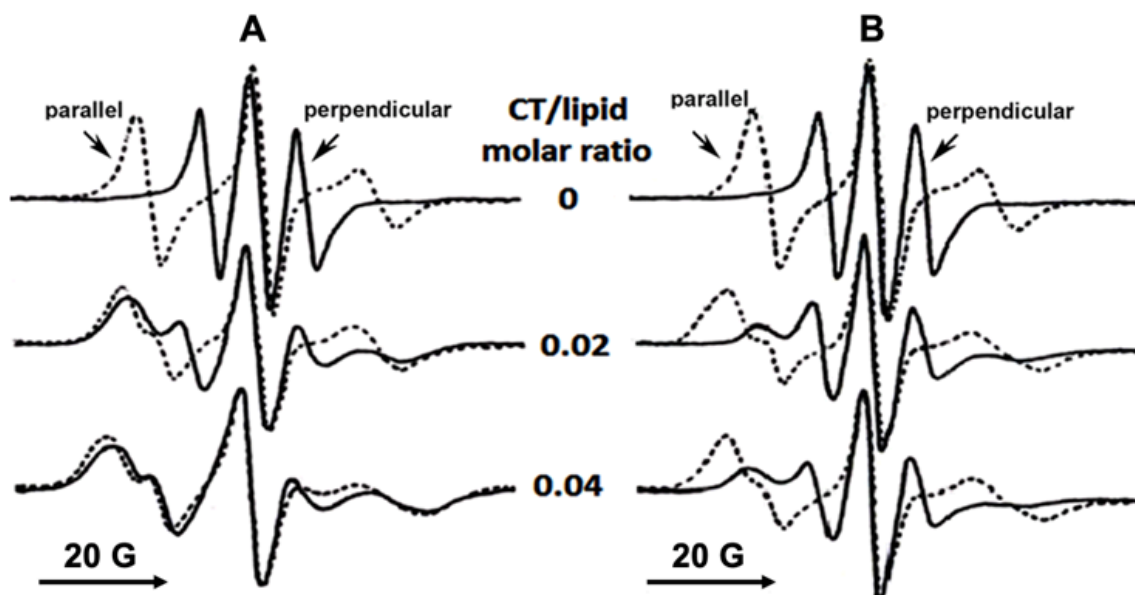


**Figure 4.** 5-DSA EPR spectra in lipid films of PC+10 mol% PS treated with cytotoxin CTII (A) or cytotoxin CTI (B) at the indicated CT/lipid molar ratios. 5-DSA: lipid molar ratio is 1:100. The bilayer normal that is parallel or perpendicular to the magnetic field is indicated by arrows at the respective EPR resonance lines. This figure is modified from [\[13\]](#).

For quantitative analysis of the changes in EPR spectral lines derived from the oriented lipid films, the EPR spectra are processed in terms of the order parameter  $S$  [\[20\]\[24\]\[25\]\[26\]](#) and the  $B/C$  ratio [\[22\]\[24\]\[25\]\[26\]](#). The  $B/C$  ratio reflects the macroscopic packing order and morphological arrangement of lipids in membrane. The  $B/C$  ratio values between 0.7 to 0.8 reflect a highly ordered packing of lipids in a lamellar phase [\[20\]\[22\]](#) and  $B/C$  ratio values below 0.4 strongly suggest transition to non-bilayer lipid phase [\[13\]\[20\]\[22\]](#). As one can see from data shown in Figure 5, cytotoxin CTI did disturb lipid films made of PC+PS but was not able to trigger the transition from lamellar phase to non-bilayer phase. In all other lipid films both cytotoxins CTI and CTII triggered transition from bilayer phase to non-bilayer phase at the cytotoxin to lipid molar ratios 0.02 and above.

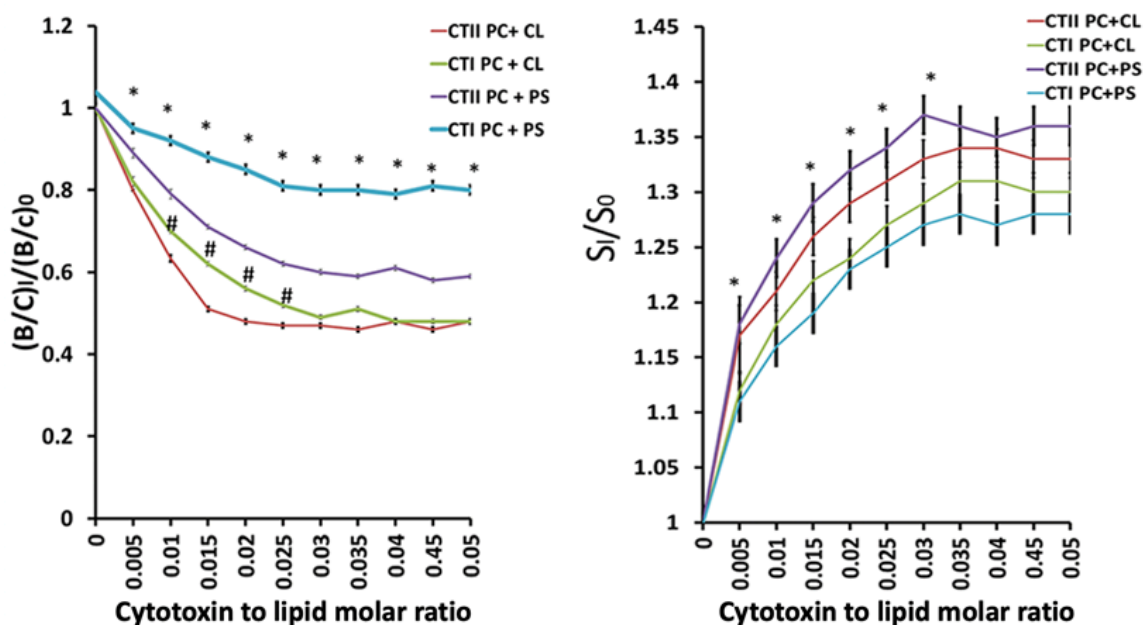


**Figure 5.** The  $B/C$  ratio (graph on the left) and parameter  $S$  (graph on the right) values processed from the oriented lipid films containing 5-DSA at molar 5-DSA to lipid ratio 1: 100 as the function of cytotoxin concentration. The graphs show the means and standard errors compiled from three independent experiments for each data point (\*:  $p$  values < 0.05 for PC+PS/CTII vs PC+PS/CTI; #:  $p$  values < 0.05 for PC+CL/CTII vs PC+CL/CTI). Values for terms  $(B/C)_0$  and  $S_0$  represent values from lipid films in absence of cytotoxins. Values for terms  $(B/C)_1$  and  $S_1$  represent values from lipid films treated at indicated cytotoxin to lipid molar ratios. This figure is modified from [13].

Parameter  $S$  reflects the changes in dynamics of lipids in membrane and is particularly sensitive to changes in rotational movement of doxyl-stearic acids [20][22]. Increase in value of parameter  $S$  reflects decrease in rate of rotation of doxyl-stearic acids resulting from immobilization of spin label movement [22][26]. Carboxyl group of DSA is negatively charged at neutral pH so DSA models behavior of acidic lipids in membrane. As one can see from the graphs on Figure 5 both cytotoxins CTI and CTII induced increase in value of parameter  $S$  in lipid films containing either CL and or PS. It was suggested that increase in parameter  $S$  shown in Figure 5 reflects interaction of basic cytotoxins with acidic lipids resulting in decrease of rotational movement of acidic lipids [13]. Overall, the results shown in Figures 4 and 5 suggest that cytotoxins interact with lipid films to immobilize acidic phospholipids and in the PC lipid films containing 10mol% of CL both cytotoxins trigger bilayer to non-bilayer phase transition [13].

## Differential scanning microcalorimetry

Differential scanning microcalorimetry (DSMC) has been used to study the order of packing of lipids in a liquid-crystalline membrane and the effects of membrane-active proteins on the packing order of lipids in membrane by recording membrane thermograms and assessing the melting cooperativity of lipids [\[11\]\[12\]\[13\]\[27\]\[28\]\[29\]\[30\]\[31\]](#). DSMC has been also used for studying intermembrane exchange of lipids [\[20\]\[21\]](#) and membrane fusion [\[11\]\[12\]\[13\]\[32\]](#) – molecular rearrangement events triggered by transition from bilayer to non-bilayer phase [\[11\]\[13\]\[14\]\[15\]\[19\]](#).

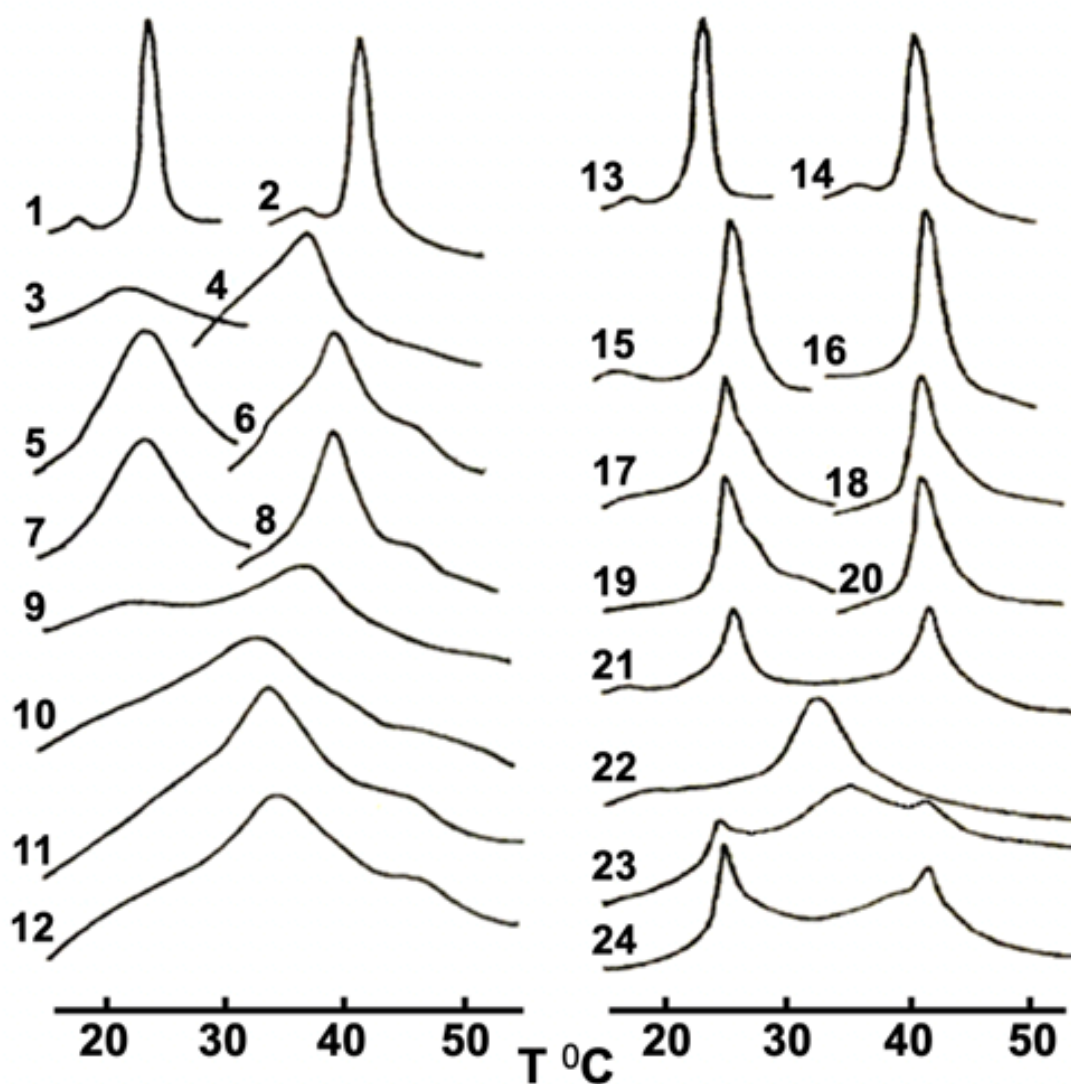


**Figure 6.** Thermograms of dimyristoylphosphatidylcholine (DMPC) – curves 1 and 13; dipalmitoyl phosphatidylcholine (DPPC) – curves 2 and 14; DMPC+5 mol% CL – curve 3; DPPC+5 mol% CL – curve 4; DMPC + 5mol% CL + CTII – curve 5; DPPC + 5 mol% CL + CTII – curve 6; DMPC + 5 mol% CL + CTI – curve 7; DPPC + 5mol% CL + CTI – curve 8; mixture of DMPC + 5 mol% CL and DPPC + 5 mol% CL – curve 9; mixture 9 after sonication – curve 10; mixture 9 + CTII – curve 11; mixture 9 + CTI – curve 12; DMPC + 10 mol% dimyristoylphosphatidylserine (DMPS) – curve 15; DPPC + 10 mol% DPPS – curve 16; DMPC + 10 mol% DMPS + CTII – curve 17; DPPC + 10 mol% DPPS + CTII – curve 18; DMPC + 10 mol% DMPS + CTI – curve 19; DPPC + 10 mol% DPPS + CTI – curve 20; mixture of DMPC + 10 mol% DMPS and DPPC + 10 mol% DPPS – curve 21; mixture 21 after sonication – curve 22; mixture 21 + CTII – curve 23; mixture 21 + CTI – curve 24. The CT/lipid molar ratio was 0.02 in all experiments involving treatment with CTs. This figure was modified from [13].

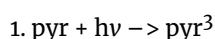
A bilayer phase of pure saturated lipids of same species has a high degree of melting cooperativity as all lipids transition from solid to liquid phase within a narrow temperature range [27]. Calorimetric curve of a lipid phase made of pure saturated lipids of same species has a characteristic thermogram line with a narrow peak at a temperature of solid-liquid phase transition (melting point) and a small pretransition peak located 5 to 10 °C below the main transition peak [32]. Temperature of the main transition is different for different saturated lipids as it depends on the length of lipid alkyl chains and the physico-chemical properties of lipid polar heads such as charge or degree of polarity [11][27]. Calorimetric curves of two samples of liposomes, one made of dimyristoylphosphatidylcholine, DMPC, and another of dipalmitoylphosphatidylcholine, DPPC, each has a pretransition peak and a main narrow transition peak with the temperature difference between main transition peaks of about 18°C (Figure 6, curves 1, 2, 13 and 14). Inclusion of 5 mol% CL into each of two types of liposomes dramatically decreases the melting cooperativity of lipids as shown by widening of the calorimetric curves and shifting the calorimetric peaks to lower temperatures (Figure 6, curves 3 and 4). The effect of inclusion of CL on a shape of calorimetric curve is more significant with DMPC+CL liposomes than that with DPPC+CL liposomes that could be explained by the shorter alkyl chains of DMPC compared to DPPC – the lipid packing order is more susceptible to external effects for lipids with the shorter alkyl chains (Figure 6, curve 3). Treatment of DMPC+CL liposomes with either CTII (Figure 6, curves 5 and 6) or CTI (Figure 6, curves 7 and 8) enhanced the lipid melting cooperativity as the basic cytotoxins induced segregation of acidic CL molecules freeing areas of pure DMPC or DPPC. A thermogram of a mixture of the DMPC+CL and DPPC+CL liposomes showed two broad peaks with individual maximums coinciding with the transition temperatures of curves 3 and 4 in Figure 6 which points to the absence of inter-liposomal exchange of lipids. When these two populations of liposomes were sonicated, calorimetric curve had a single-phase transition peak (Figure 6, curve 10) with the maximum at a temperature in the middle between transition peaks of DMPC+CL and DPPC+CL liposomes. This observation suggests the lipids from the two population of liposomes are completely mixed in a single set of liposomes. Very similar results were obtained when these two populations of liposomes were treated with either CTII (Figure 6, curve 11) or CTI (Figure 6, curve 12) with the only difference that the thermograms in curves 11 and 12 very sharper than that in curve 10 that strongly suggests cytotoxin-induced segregation of CL molecules. In addition, the single-phase transition peaks in curves 11 and 12 is the results of a thorough mixing of DMPC and DPPC molecules in the one set of liposomes which is the outcome of the cytotoxin-induced fusion of liposomes [18][12][13][19].

Inclusion of 10 mol% dimyristoylphosphatidylserine (DMPS) and 10 mol% dipalmitoylphosphatidylserine (DPPS) into DMPC and DPPC liposomes respectively (see curves 15 and 16 in Figure 6) inflicted much lower effects on lipid packing and shape of thermograms (see pure DMPC and DPPC curves 13 and 14 in Figure 6) compared to the effects of CL. This is because natural CL has four unsaturated alkyl chains while DMPS and DPPS are synthetic lipids each with two saturated alkyl chains with the same length as DMPC and DPPC respectively. For these reasons, DMPS and DPPS respectively disturb membranes of DMPC and DPPC liposomes to much lesser extent than CL. Treating these liposomes with CTII (Figure 6, curves 17 and 18) or CTI (Figure 6, curves 19 and 20) shifted the peaks of phase transitions to the phase transitions peaks in curves 13 and 14 (Figure 6) strongly pointing to the cytotoxin-induced segregation of acidic DMPS and DPPS. Mixing the two samples of liposomes resulted in the two peaks thermogram with the phase transitions peaks coinciding with that in curves 15 and 16 (Figure 6) which points to the absence of inter-liposomal exchange of lipids. The shape of thermogram in curve 22 (Figure 6) derived from sonication of two population of liposomes points to the thorough mixing of lipids that produced one population of liposomes. Treatment of a mixture of two population of liposomes with CTII resulted in thermogram with two peaks coinciding with the phase transition peaks in curves 13 and 14 and a broad peak in a middle (Figure 6, curve 23). This thermogram strongly suggests that CTII induces segregation of acidic phospholipids and fusion of about 60% of liposomes (judging from the area of the middle peak). The shape of thermogram derived from the treatment of two population of liposomes with CTI (Figure 6, curve 24) strongly suggests that CTI induces segregation of acidic lipids but does not induce fusion of liposomes. Thus, this DSC study showed that both cytotoxins induce segregation of acidic lipids, CL, DMPS or DPPS, but only CTII is capable of inducing fusion of liposomes with either CL or phosphatidylserine, while CTI can induce fusion of only liposomes containing CL. CL with four alkyl chains and a sharply angled conical shape has the highest non-bilayer propensity of all lipids. Increasing CL content in membranes increases membrane fusibility<sup>[14]</sup> which together with the high non-bilayer propensity of CL suggests that membrane fusion is mediated by formation of non-bilayer lipid structures.

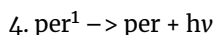
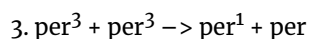
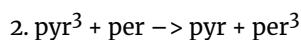
## Luminescent spectroscopy in studies of intermembrane lipid exchange and membrane fusion

The quenching of erythrosine phosphorescence induced by clashes with ferrocene is a commonly used method for assessing changes in membrane fluidity <sup>[13][28][33]</sup>. Erythrosine in membrane is located in area of polar lipid heads <sup>[13][34]</sup> and ferrocene in membrane is located in the interface between polar heads and alkyl chains <sup>[34]</sup>. Because of proximity of locations of both erythrosine and ferrocene to the membrane surface, the quenching of erythrosine phosphorescence induced by clashes with ferrocene was used for studies of intermembrane exchange of lipids between two liposome populations, one population containing erythrosine and another population containing ferrocene <sup>[34]</sup>. When two population of liposomes, one with erythrosine and another with ferrocene, were mixed, no quenching of erythrosine phosphorescence was observed which indicated on absence of clashes between erythrosine and ferrocene and thus absence of lipids exchange between two populations of liposomes <sup>[34][35]</sup>. However, treatment of liposomes made of PC+10mol% CL or PC+10 mol% PS with either CTI or CTII has triggered quenching of erythrosine phosphorescence which was a result of effective clashes between erythrosine and ferrocene facilitated by intermembrane exchange of lipids between of two populations of liposomes <sup>[34]</sup>.

The emission of annihilated retarded fluorescence (ARF) takes place when chromophores excited at a triplet state collide which leads to one molecule relaxing to the basic state and another molecule getting excited to the singlet state <sup>[33]</sup>. The ARF emission was observed with polycyclic aromatic hydrocarbon chromophores pyrene and perylene which are located deep in hydrophobic area of membrane <sup>[35]</sup>. When either pyrene or perylene at low concentration is irradiated by a laser with insufficient excitation power, no ARF is observed, but when pyrene and perylene are mixed at low concentrations a high intensity fluorescence with a lifetime of  $4.5 \times 10^{-5}$  s is observed even at an insufficient excitation power of laser <sup>[35]</sup>. This phosphorescence is facilitated by the triplet-triplet energy transfer. Pyrene has a higher triplet energy level than perylene which allows efficient transfer of energy from the excited triplet level of pyrene to the triplet level of perylene  $\text{pyr}^3 + \text{per} \rightarrow \text{pyr} + \text{per}^3$ ; thus pyrene acts as a sensitizer of the retarded fluorescence of perylene {m/64-66/}. The steps of this process can be described as follows:







This phenomenon of the sensitized triplet-triplet transfer of energy between pyrene and perylene has been used to study membrane fusion triggered by cytotoxins [11][36]. A sample of two populations of liposomes with low concentrations of chromophores, one with pyrene and another with perylene, were mixed and no luminescence was observed. When this sample was sonicated to fuse liposomes a fluorescence with a lifetime of  $4.5 \times 10^{-5}$  s was observed [11][36]. Using this sensitized triplet-triplet transfer of energy method in two populations of liposomes with different chromophores it was determined that CTII triggers the fusion of PC+10 mol% CL and PC+10mol% PC liposomes while CTI was able to trigger the fusion of only PC+10 mol% CL liposomes [35][36]. Non-bilayer lipid structures were observed by  $^{31}\text{P}$ -NMR,  $^1\text{H}$ -NMR and EPR of 5-DSA in oriented PC+CL films treated with CTII and CTI [13][14][15][21]. This strongly suggests that fusion of CL containing membranes is mediated by formation of non-bilayer lipid structures.

## Conclusions

The plethora of powerful physical methods of analysis which are being used in studies of polymorphic transitions of lipids in model and biological membranes provides not only the strong evidence for existence of non-bilayer lipid structures in model and biological membranes, but also allows one to conclude that non-bilayer structures mediate important functions of biological membranes. It is important that in the studies of lipid polymorphism in membrane systems the researchers use as many various physical methods as possible because various methods complement each other as each method provides the specific information limited to the capability of a particular method. Using various physical methods at solving one problem allows researchers to obtain a broader picture about the object under investigation. We believe that this review, which is focused on application of various powerful physical methods in studies of dynamic structure of biological membranes, will attract more attention of experts in membranology toward the studies on elucidation of the roles of non-bilayer phases that should lead to better understanding of fundamental mechanisms that drive functional activities of biological membranes.

**Author Contributions:** The work was initiated by E.S.G. and M.L. has conducted research studies on relevant literature published over the last 60 years. E.S.G. has written the first draft of the manuscript and M.L. contributed extensively by reviewing and editing the manuscript. Both authors participated in the final editing of the manuscript and agreed to the published version of the manuscript.

**Funding:** This research was funded by the CKWA start-up grant to the STEM Research Center.

**Conflicts of Interest:** The authors declare no conflict of interest.

## References

1. <sup>△</sup>Seddon, J.M.; Templer, R.H. Polymorphism of lipid-water systems, In *Handbook of Biological Physics*, Lipowsky, R., Sackmann E., Eds.; North-Holland 1995, pp. 97–160.
2. <sup>△</sup>Luzzati, V.; Spegt, P.A. Polymorphism of lipids. *Nature* 1967, 215(5102), 701–704.
3. <sup>△</sup>Luzzati, V.; Tardieu, A. Lipid phases: structure and structural transitions. *Annu Rev Phys Chem* 1974, 25 (1), 79–94.
4. <sup>△</sup>Rand, R.P.; Sengupta, S. Cardiolipin forms hexagonal structures with divalent cations. *Biochim Biophys Acta* 1972, 255(2), 484–492.
5. <sup>△</sup>Shipley, G.G.; Green, J.P.; Nichols, B.W. The phase behavior of monogalactosyl, digalactosyl, and sulpho quinosyl diglycerides. *Biochim Biophys Acta* 1973, 311(4), 531–544.
6. <sup>△</sup>Williams, W.P.; Brain, A.P.R.; Dominy, P.J. Induction of nonbilayer lipid phase separations in chloroplast thylakoid membranes by compatible co-solutes and its relation to the thermal-stability of photosystem-II. *Biochim Biophys Acta* 1992, 1099(2), 137–144.
7. <sup>△</sup><sup>‡</sup>Semenova, G.A. The relationship between the transformation of thylakoid acyl lipids and the formation of tubular lipid aggregates visible on fracture faces. *J Plant Physiol* 1999, 155(6), 669–677.
8. <sup>△</sup>de Kruijff, B.; Morris, G.A.; Cullis, P.R. Application of P-31-NMR saturation transfer techniques to investigate phospholipid motion and organization in model and biological membranes. *Biochim Biophys Acta* 1980, 598(1), 206–211.
9. <sup>△</sup>Medina-Carmona, E.; Varela, L.; Hendry, A.C.; Thompson, G.S.; White, L.J.; Boles, J.E.; Hiscock, J.R.; Ortega-Roldan, J.L.; A quantitative assay to study the lipid selectivity of membrane-associated systems using solution NMR. *Chem Commun (Camb)* 2020, 56(78), 11665–11668.
10. <sup>△</sup><sup>‡</sup>Cullis, P.R.; de Kruijff, B. Lipid polymorphism and the functional roles of lipids in biological membranes. *Biochim Biophys Acta* 1979 559(4), 399–420.

11. <sup>a, b, c, d, e, f, g, h</sup>Eicher, B.; Marquardt, D.; Heberle, F.A. Intrinsic curvature-mediated transbilayer coupling in asymmetric lipid vesicles. *Biophys J* 2018, 114, 146–157.
12. <sup>a, b, c, d, e, f, g, h, i, j, k</sup>Feofanov, A.V.; Sharonov, G.V.; Astapova, M.V.; Rodionov, D.I.; Utkin, Y.N.; Arseniev, A.S. Cancer cell injury by cytotoxins from cobra venom is mediated through lysosomal damage. *Biochem J* 2005, 390, 11–18.
13. <sup>a, b, c, d, e, f, g, h, i, j, k, l, m, n, o, p, q, r, s, t</sup>Gasanov, S.E.; Shrivastava, I.H.; Israilov, F.S.; Kim, A.A.; Rylova, K.A.; Zhang, B.; Dagda, R.K. Naja naja oxiana cobra venom cytotoxins CTI and CTII disrupt mitochondrial membrane integrity: implications for basic three-fingered cytotoxins. *PLoS One* 2015, 10(6), e0129248. doi:10.1371/journal.pone.0129248
14. <sup>a, b, c, d, e</sup>Li, F.; Shrivastava, I.H.; Hanlon, P.; Dagda, R.K.; Gasanoff, E.S. Molecular mechanism by which cobra venom cardiotoxins interact with the outer mitochondrial membrane. *Toxins (Basel)* 2020, 12(7), 425.
15. <sup>a, b, c, d</sup>Gasanov, S.E.; Kim, A.A.; Yaguzhinsky, L.S.; Dagda, R.K. Non-bilayer structures in mitochondrial membranes regulate ATP synthase activity. *Biochim Biophys Acta* 2018, 1860(2), 586–599.
16. <sup>a, b</sup>Seelig, J. Deuterium magnetic resonance: theory and application to lipid membranes. *Q Rev Biophys* 1977 10(3), 353–418.
17. <sup>a</sup>Mantsch, H.; Saito, H.; Smith, I. Deuterium magnetic resonance, applications in chemistry, physics and biology. *Prog Nuc Mag Res Spec* 1977, 11(4), 211–72.
18. <sup>a, b</sup>Kalita, B.; Utkin, Y.N.; Mukherjee, A.K. Current insights in the mechanisms of cobra venom cytotoxins and their complexes in inducing toxicity: implications in antivenom therapy. *Toxins* 2022, 14, 839. <https://doi.org/10.3390/toxins14120839>.
19. <sup>a, b, c</sup>Baker, C.D.; Ball, W.B.; Erin N. Pryce, E.N.; Gohil, V.M. Specific requirements of nonbilayer phospholipids in mitochondrial respiratory chain function and formation. *Mol Biol Cell* 2016, 27, 2161–2171.
20. <sup>a, b, c, d, e, f</sup>Dubinnyi, M.A.; Dubovskii, P.V.; Utkin, Y.N. et al. An ESR study of the cytotoxin II interaction with model membranes. *Russian Journal of Bioorganic Chemistry* 2001, 27, 84–94. <https://doi.org/10.1023/A:1011329002584>
21. <sup>a, b, c</sup>Gasanov, S.E.; Kim, A.A.; Dagda, R.K. The possible role of nonbilayer structures in regulating ATP synthase activity in mitochondrial membranes. *Biophysics (Oxf)* 2016, 61(4), 596–600.
22. <sup>a, b, c, d, e, f</sup>Berliner, L.J. *Methods of spin labels*. Mir: Moscow, USSR. 1979.
23. <sup>a, b</sup>Devaux, P.F.; Seigneuret, M. Specificity of lipid-protein interactions as determined by spectroscopic techniques. *Biochim Biophys Acta*. 1985, 822(1), 63–125.

24. <sup>a, b</sup>Gasanov, S.E.; Alsarraj, M.A.; Gasanov, N.E.; Rael, E.D. Cobra venom cytotoxin free of phospholipase A<sub>2</sub> and its effect on model membranes and T leukemia cells. *J Membr Biol* 1997, 155, 133–142.
25. <sup>a, b</sup>Gasanov, S.E.; Gasanov, N.E.; Rael, E.D. Phospholipase A<sub>2</sub> and cobra venom cytotoxin Vc5 interaction and membrane structure. *Gen Physiol Biophys* 1995, 14, 107–123.
26. <sup>a, b, c</sup>Gasanoff, E.S.; Liu, Y.; Li, F.; Hanlon, P.; Garab, G. Bee venom melittin disintegrates the respiration of mitochondria in healthy cells and lymphoblasts, and induces the formation of non-bilayer structures in model inner mitochondrial membranes. *Int. J. Mol. Sci.* 2021, 22, 11122.
27. <sup>a, b, c</sup>Ivanov, I. Calorimetric methods of studying biopolymers and membrane systems. In *Modern Methods of Biophysical Investigations – a Practicum of Biophysics*, Rubin, V.A., Ed.; Vyshaya Shkola: Moscow, USSR, 1988, 203–216.
28. <sup>a, b</sup>Li, J.; Hanlon, P.; Gasanoff, E.S. Interaction of bee venom melittin, a potential anti-cancer drug, with phosphatidylcholine membrane enriched with phosphatidylserine. *EC Pharmacology and Toxicology* 2020, 8.11, 119–129.
29. <sup>a</sup>Gasanov, S.E.; Rael, E.D.; Gasanov, N.E.; Vernon, L.R. In vitro evaluation of Pyrularia thionin-anti-CD5 immunotoxin. *Cancer Immunol Immunother* 1995, 41, 122–128.
30. <sup>a</sup>Xu, Y.; Hanlon, P.; Rael, E.D.; Gasanoff, E.S. Bee venom melittin modulates phospholipase A<sub>2</sub> activity by affecting substrate interface on the surface of phosphatidylcholine membrane. *Ann Toxicol* 2020, 2(1), 26–35.
31. <sup>a</sup>Talbot, J.C.; Bernard, E.; Maurel J.P.; Faucon J.F.; Dufourcq, J. Melittin-phospholipid interactions: binding of the mono- and tetrameric form of this peptide, and perturbations of the thermotropic properties of bilayers. *Toxicon* 1982, 20(1), 199–202. doi: 10.1016/0041-0101(82)90193-3.
32. <sup>a, b</sup>Papahadjopoulos, D.; Portis A.; Pangborn, W. Calcium-induced lipid phase transitions and membrane fusion. *Ann. N. Y. Acad. Sci.* 1978, 308, 50–66.
33. <sup>a, b</sup>Parker, C. *Solution Photoluminescence*, Mir: Moscow, USSR, 1972.
34. <sup>a, b, c, d, e</sup>Mekler, V.M.; Kotelnikov, A.I.; Lichtenshtein, G.I.; Berkovich, M.A. (1982): Application of phosphorescent probes for the study of model and biological membranes. *Biofizika* 1982, 27, 641–645.
35. <sup>a, b, c, d</sup>Mekler, V.M.; Kotelnikov, A.I.; Lichtenshtein, G.I. Application of probes emitting annihilation retarded fluorescence for studies of model and biological membranes. *Biofizika* 1983, 28, 303–305.
36. <sup>a, b, c</sup>Aizawa, N.; Pu, Y.J.; Harabuchi, Y. et al. Delayed fluorescence from inverted singlet and triplet excited states. *Nature* 2022, 609, 502–506. <https://doi.org/10.1038/s41586-022-05132-y>

## **Declarations**

**Funding:** No specific funding was received for this work.

**Potential competing interests:** No potential competing interests to declare.